

On the dynamical mechanism of mid-latitude jet stream variability and annular modes

JOE KIDSTON *

NATIONAL INSTITUTE OF WATER AND ATMOSPHERIC RESEARCH,

AND

SCHOOL OF GEOGRAPHY, EARTH AND ENVIRONMENTAL SCIENCES,

VICTORIA UNIVERSITY OF WELLINGTON

WELLINGTON, NEW ZEALAND

D. M. W. FRIERSON

UNIVERSITY OF WASHINGTON, SEATTLE, U.S.A.

J. A. RENWICK

NATIONAL INSTITUTE OF WATER AND ATMOSPHERIC RESEARCH,

WELLINGTON, NEW ZEALAND

* *Corresponding author address:* Joe Kidston, Private Bag 14901, NIWA, Wellington, New Zealand.

ABSTRACT

We examine the characteristics of the leading mode of extra-tropical variability (the so-called annular modes) in the context of the recent theory that eddy-driven jets may be self-maintaining. We show that the leading mode of variability is associated with changes in the eddy source latitude, and that the latitude of the eddy source region is organised by the mean flow. This is consistent with the idea that the annular modes should be thought of as the meridional wandering of a self-maintaining jet, and that a positive baroclinic feedback prolongs these vacillations. Further, the degree to which the eddy-driven flow is self-maintaining determines the time-scale of the leading mode in a simplified general circulation model. Preliminary results indicate that the same dynamics are important in the real atmosphere.

1. Introduction

The leading mode of atmospheric variability in the extra-tropics of both hemispheres is the meridional vacillation of the equivalent barotropic eddy-driven jet streams and embedded storm tracks (Kidson 1988; Mo and White 1985; Thompson and Wallace 2000; Baldwin 2001; Wallace 2000). This variability is variously referred to as the annular modes (Limpasuvan and Hartmann 1999), the Antarctic or Arctic oscillations (Thompson and Wallace 1998; Gong and Wang 1999) the Pacific North American mode (Wallace and Thompson 2002; Matsueda and Tanaka 2005), and the North Atlantic oscillation (Visbeck et al. 2001; Ambaum et al. 2001; Huth 2007). Here, we use the terminology “annular modes.” It is a matter of ongoing debate whether such a mode represents hemispherically coherent variability, or is simply due to localised dynamics (e.g. Thompson et al. (2003)). These modes are the dominant drivers of mid-latitude temperature and precipitation variability at seasonal and inter-annual time-scales (Hurrell et al. 2003; Marshall et al. 2001; Gillett et al. 2006; Thompson and Wallace 2001).

The principal response in the mid-latitudes to increasing atmospheric concentrations of greenhouse gasses (GHGs) is projected to be a poleward shift of the storm-tracks, which is a positive trend in the annular modes (Meehl et al. 2007; Yin 2005; Kushner et al. 2001; Bengtsson et al. 2006; Miller et al. 2006). It has been suggested that differences among general circulation models (GCMs) in the magnitude of the projected poleward shift of the eddy-driven jet stream due to increasing GHGs may be related to the variability of the annular modes by fluctuation-dissipation theory. A larger poleward shift is associated with more persistent annular modes in the control runs (Ring and Plumb 2007). Hence

understanding the controlling mechanism on annular mode time-scales in GCMs may enable improved quantitative assessment of projections for future climate changes.

To first order in the quasi-geostrophic (QG) framework and ignoring the sphericity of the Earth, the equations that describe the zonal-mean zonal momentum balance (away from the Earth’s surface) and mass continuity are

$$\frac{\partial \bar{u}}{\partial t} - f \bar{v} = -\frac{\partial}{\partial y} \overline{u'v'} \quad (1a)$$

$$\frac{\partial \bar{\omega}}{\partial p} + \frac{\partial \bar{v}}{\partial y} = 0 \quad (1b)$$

where u , v , and ω respectively refer to the zonal, meridional, and pressure velocity, f is the Coriolis parameter, primes denote departures from the zonal mean and the overbar represents zonal averaging. The R.H.S. of (1a) is the convergence of the meridional eddy momentum flux. It is clear that if the large scale flow organises the eddy momentum flux convergence so that $\frac{\partial \bar{u}}{\partial t} > 0$ where \bar{u} is maximum then a positive feedback exists, and any latitudinal displacement of the mean flow may be enhanced, leading to the dominance of annular modes over other variability. Numerous authors have suggested that such a feedback is important (Robinson 1994, 1996; Limpasuvan and Hartmann 2000; Lorenz and Hartmann 2001, 2003; Gerber and Vallis 2007). There have been various mechanisms proposed for this feedback. Hartmann and co-authors first proposed a barotropic mechanism, whereby the meridional shear of the westerlies is crucial for determining the lifecycle of the eddies (e.g. Hartmann (2000)). Specifically, when the jet is displaced poleward, there is increased anticyclonic shear on the equatorward flank, which encourages anticyclonic, or LC1 type (Thorncroft et al. 1993) wavebreaking, which tends to reinforce the existing wind-speed anomaly. This can be argued from the refractive index (n^2) viewpoint (Limpasuvan and Hartmann 2000). The refractive

index is anomalously low at high latitudes when the annular modes are positive, and so waves (which propagate towards high n^2) propagate preferentially equatorward. The momentum flux convergence associated with equatorward wave propagation tends to further reduce n^2 at high latitudes. Alternatively, from the potential vorticity (PV) point of view, when the jet is displaced equatorward, the relatively weak PV gradient on the poleward flank of the jet encourages increased cyclonic, or LC2 wavebreaking (Hartmann 1995), and the associated momentum flux convergence prolongs the equatorward displacement of the jet.

Other mechanisms have been suggested that are baroclinic. The primary source of large-scale eddy activity in the atmosphere is baroclinic instability. The barotropic westerlies arise due to the meridional propagation of eddies aloft, away from their source region. In quasi-steady state the main sink for the resulting convergence of westerly momentum flux is friction near the surface, necessitating a barotropic eddy-driven jet stream (Held 1975). If there exists a self-maintaining mechanism whereby baroclinic eddies tend to be born at the latitude of the eddy-driven jet, then their meridional transport of momentum tends to prevent the jet from shifting latitudes. If this negative feedback on the jet movement were very strong, the jet may never move, but if the latitude of the jet is subject to stochastic variability, then a positive baroclinic feedback would tend to prolong any displacement.

Robinson (2000, 1996, 1994) has suggested that such a feedback arises due to surface drag. Friction at the surface acts on the barotropic increase in wind-speed associated with the eddy life-cycle (Simmons and Hoskins 1978) to increase the vertical shear of the westerly wind, providing a low-frequency feedback that tends to generate baroclinic instability at the core of the eddy-driven jet.

Another baroclinic feedback mechanism, also suggested by Robinson (2006) focuses on

the upper level Eliassen-Palm (EP) flux divergence. In the transformed Eulerian mean (T.E.M. reference? Andrews) framework (1a) and (1b) become

$$\frac{\partial \bar{u}}{\partial t} - f \bar{v}^* = -\nabla \cdot \vec{F} \quad (2a)$$

$$\frac{\partial \bar{\omega}^*}{\partial p} + \frac{\partial \bar{v}^*}{\partial y} = 0 \quad (2b)$$

where the variables with the * superscript are transformed Eulerian mean quantities, and can be thought of as thickness-weighted versions of their Eulerian counterparts (Edmon et al. 1980; Vallis 2006). $\bar{\omega}^*$ takes account of the fact that an eddy heat flux convergence results in upward Eulerian motion simply because thicker air masses converge in the Eulerian averaging space. Thus the Eulerian vertical velocity may be non-zero even though no individual air parcel rises or falls. In the QG framework $\nabla \cdot \vec{F}$ represents the total zonal force exerted by the eddies on the mean flow; the meridional component of $\nabla \cdot \vec{F}$ is the R.H.S of (1a), and the vertical component of $\nabla \cdot \vec{F}$ is $\frac{\partial}{\partial p} \frac{\overline{v'\theta'}}{\theta_p} f$, where θ is the potential temperature. $\frac{\partial}{\partial p} \frac{\overline{v'\theta'}}{\theta_p} f$ is the convergence of the vertical momentum flux that is inherent to a meridional eddy heat flux and the form drag due to the westward phase tilt with height required by hydrostatic balance. The T.E.M. represents a more Lagrangian view of fluid motion. $\nabla \cdot \vec{F}$ is generally negative in the upper atmosphere (Edmon et al. 1980; Holton 1992; Vallis 2006), indicative that even at the core of the storm track, where the meridional propagation of eddies gives $-\frac{\partial}{\partial y} \overline{u'v'} > 0$, the form drag term $\frac{\partial}{\partial p} \frac{\overline{v'\theta'}}{\theta_p} f < 0$ and dominates.

However, a subtle but important point arises if $-\frac{\partial}{\partial y} \overline{u'v'}$ is large enough in magnitude that there is a local maximum in $\nabla \cdot \vec{F}$ at the core of the jet. Then $\nabla \cdot \vec{F}$ is less negative at the core of the jet than on the flanks. If this is true (and $\nabla \cdot \vec{F}$ in the lower layers exhibits

a broad maximum characteristic of the heat flux term) then it can be said that the eddies decrease the vertical shear (and so the baroclinic instability) more effectively on the flanks of the jet than at the core, and so incremental shifts in the latitude of the jet are discouraged (Gerber and Vallis 2007).

An equivalent way of expressing this feedback comes from the understanding that in quasi-steady state $\bar{v}^* = -\frac{1}{f}\nabla \cdot \vec{F}$. (Note that $\nabla \cdot \vec{F} < 0$ requires that \bar{v}^* is poleward in the upper troposphere, and the Ferrell cell disappears in the T.E.M., so that to first order the thickness-weighted overturning is a single thermally direct cell in each hemisphere). Thus a local maximum in $\nabla \cdot \vec{F}$ at the storm track means that \bar{v}^* will have a local minimum, so that on the poleward flank $\frac{\partial \bar{v}^*}{\partial y} > 0$. By (2b) this must be associated with $\frac{\partial \bar{\omega}^*}{\partial z} < 0$. Because the primary momentum sink is friction near the surface, this circulation must close downwards (Haynes et al. 1991), giving rising and adiabatic cooling on the poleward flank. The same reasoning gives sinking and warming on the equatorward flank. This thermally indirect motion increases the meridional temperature gradient (and so the baroclinic instability) at the core of the storm track relative to elsewhere (Robinson 2006). It has been suggested by Gerber and Vallis (2007) that this provides a negative feedback on the meridional vacillation of an eddy-driven jet stream, thereby prolonging displacements of the jet, and causing that mode of variability to be dominant.

Here we develop the ideas of Robinson (2006) and Gerber and Vallis (2007) and argue that the low-frequency meridional vacillation of an eddy-driven jet stems from a baroclinic feedback. We first show that the annular modes are inherently baroclinic in nature. A simplified GCM is then used to show that the time scale of the annular mode is determined by the magnitude of the baroclinic feedback described above. We also analyse observational

data and argue that this mechanism is important in the real atmosphere.

2. Data and Methods

The data from the NCEP/NCAR reanalysis project are utilized (Kalnay et al. 1996). Only data from 1979-2007 are included due to the lower quality of the pre-satellite-era analyses. The dry baroclinic dynamical core developed at the Geophysical Fluid Dynamics Laboratory is used as a simplified GCM. The model is a spectral model with truncation at T42, and 20 levels evenly spaced in fraction of surface pressure (σ), as described in Held and Suarez (1994). The model is simplified in that the only forcings are Newtonian cooling, Rayleigh friction (below $\sigma = 0.7$) and hyperdiffusivity to remove energy at small scales. The model forcings are hemispherically and zonally symmetric and steady in time. The primitive hydrostatic momentum equations are solved on the sphere, giving some confidence that large-scale dynamics relate to the real atmosphere. After a spinup period of 400 days the model was integrated for 1600 days per run. In the control run the model parameters were as in Held and Suarez (1994); the Equator-Pole equilibrium temperature (T_{eq}) difference was 60K, the e -folding period for the linear drag operator at the surface was 1 day, T_{eq} in the stratosphere was 200 K, and the hyperdiffusivity operator was ∇^8 .

For the observational data we define the climatology as the mean for the calendar month, with a 50 day low-pass 5th order Butterworth filter applied. For the model output the climatology was simply the time mean.

We define the leading mode of variability as the first empirical orthogonal function (EOF, reference, perhaps Wilks 1995? [JR]) of the daily zonal-mean zonal wind anomalies ($\bar{u}' =$

$\bar{u} - \bar{u}_{clim}$, the $clim$ subscript representing the climatology described above). The EOF was calculated in the meridional-height plane from the equator to the pole and u' was area weighted to allow for converging meridians. In all of the datasets, the first EOF represented a meridional vacillation of the eddy-driven jet stream, with an equivalent barotropic structure that flanks the climatological flow. E.g. in the Southern hemisphere (SH), when the annular mode is positive, $\bar{u}' > 0$ at 60S and $\bar{u}' < 0$ at 40S, with a node at the climatological maximum \bar{u} at 50S (e.g. Lorenz and Hartmann (2001)). We take the principal component of the first EOF (PC1) as the time series of the annular mode. For the observational data, PC1 was calculated without splitting the data into seasons (as in Lorenz and Hartmann (2001)). The fact that the standard deviation for each calendar month was 1 ± 0.08 is indicative of the fact that there was no clear seasonal cycle to the variability.

To investigate the degree of zonal symmetry of the variability, the ‘cross-planet cospectrum’ was calculated. At a single level, the cospectrum of u' at one longitude with u' 180 degrees of longitude away was calculated by splitting the time-series into sections of length 256 days and overlapping with the congruent sections using a Hamming window of width 128 days. In order to reduce noise, the cospectrum for each point on the latitude circle was averaged with the points at 180 ± 10 degrees of longitude away, so that the average separation was in fact 175 degrees of longitude.

As in Lorenz and Hartmann (2001, 2003) and subsequent references, a time-series of the eddy forcing of the annular mode (F) was taken as the projection of the daily meridional eddy momentum flux convergence ($-\frac{\partial}{\partial y}\overline{u'v'}$) onto the first EOF in the meridional-height plane. This was calculated for the total eddy field (F_{tot}) by taking eddy quantities as deviations from the zonal mean, and for the high-frequency eddies (F_{hf}) where eddy quantities were

calculated by applying a high-pass 5th order Butterworth filter with a 10 day cutoff. To quantify the extent to which the eddy heat flux was latitudinally displaced, we applied the same analysis to the eddy heat flux field. The daily eddy heat flux ($\overline{v'T'}$) was projected onto the first EOF in the meridional-height plane for the total eddy fields to give the time series H_{tot} . When H_{tot} is positive, there is increased eddy heat flux at 60S, and decreased eddy heat flux at 40S (these latitudes correspond to the maxima in the first EOF for the SH observations). The same analysis applied to the heat flux due to high-frequency eddies yielded the time series H_{hf} .

The eddy-driven thermally indirect vertical motion due to the meridional momentum flux convergence (\bar{w}_{eddy}) is calculated as in e.g. Seager et al. (2003). Assuming downward control, and solving (1a) and (1b) assuming a steady state gives

$$\bar{w}_{eddy} = \int_0^p -\frac{\partial}{\partial y} \frac{1}{f} \frac{\partial}{\partial y} \overline{u'v'} d\omega$$

and the hydrostatic relation is used to give the Cartesian vertical velocity $\bar{w}_{eddy} = -\frac{RT}{pg} \bar{\omega}_{eddy}$. A measure of the amount of heating attributable to this motion is given by the sum of the product of \bar{w}_{eddy} and the buoyancy frequency (N^2). We refer to this eddy-driven thermally indirect effect as $\sum \bar{w}_{eddy} N^2$. It is calculated only for the rising on the poleward flank of the jet (defined as the region where there is convergence of the eddy heat flux, $\frac{\partial}{\partial y} \overline{v'T'} < 0$, and there is rising motion, $w_{eddy} > 0$) so as to be sure to avoid any downward motion at low latitudes that may be due to a closed Hadley circulation. This is compared with the total heating on the poleward flank of the jet due to the eddy heat flux convergence

$\sum -\frac{\partial}{\partial y} \overline{v'T'}$. Because we are interested in changes between model runs, both of these metrics are normalised by the value for the control run. [should normalise it by value for control]

For convenience we have thus far written equations in the form that neglects the Earth's sphericity. For analysis purposes, calculations were made that took account of the Earth's geometry. Thus the R.H.S. of (2a) was calculated as

$$\frac{1}{a \cos(\phi)} \nabla \cdot \vec{F} = -\frac{1}{a \cos^2(\phi)} \frac{\partial}{\partial \phi} \overline{u'v' \cos^2(\phi)} + \frac{1}{a \cos(\phi)} \frac{\partial}{\partial p} \frac{\overline{v'\theta'}}{\overline{\theta_p}} f a \cos(\phi)$$

where a is the Earth's radius and ϕ is latitude. To calculate \bar{w}^* , first of all the T.E.M. vertical pressure velocity was calculated as

$$\bar{w}^* = \bar{w} + \frac{1}{a \cos(\phi)} \frac{\partial}{\partial \phi} \left(\frac{\overline{v'\theta'}}{\overline{\theta_p}} \right)$$

and converted to vertical velocity using the hydrostatic relation.

The temperature tendency due to latent heating ($\frac{\partial}{\partial t} T|_{latent}$) has been computed for the NCEP reanalysis and is provided at <http://iridl.ldeo.columbia.edu/SOURCES/.NOAA/.NCEP-DOE/.Reanalysis-2/>. We take the sum of the heating due to (i) deep convection, (ii) shallow convection and (iii) large-scale condensation.

3. Results

a. Hemispherically Symmetric Nature of the Annular Modes

The extent to which annular modes represent a genuinely hemispherically symmetric mode of variability has been a matter of some debate (Wallace 2000; Thompson et al. 2003),

and it certainly is not necessary to obtain annular leading EOFs (Cash et al. 2005; Vallis and Gerber 2008). To investigate this we examine the ‘cross-planet cospectrum’ of the zonal wind-speed anomaly (described above) shown in Fig. 1 (a). When taken as being coincident with the maximum surface westerlies, the eddy-driven jet lies at approximately 50 degrees from the Equator in both hemispheres, and so ± 60 degrees lies on the poleward flank of the jet in both hemispheres. At 60S and at low frequencies there is positive covariance between the wind-speed anomalies on opposite sides of the planet. At 50S there is no strong positive cross-planet covariance, but there is negative covariance at periods of about 30 days, presumably due to zonal wavenumber (k) = 1 variability. That there is no positive cross-planet covariance at 50S is indicative that there is no zonally-symmetric pulsing of the jet. That there is positive cross-planet covariance at 60S is indicative that the meridional vacillation of the jet is a genuinely zonally-symmetric mode of variability; even when the annular mode is in its extreme phase, the zonal-mean jet-stream encompasses the region at 50S, but when the annular mode is negative, the region at 60S may no longer correspond to the eddy-driven jet. This zonal symmetry implies that the annular mode in the SH is a result of more interesting dynamics than simple synoptic-scale stochastic forcing. Positive cross-planet covariance is also seen at 40S (not shown). A one-point correlation map in the latitude-longitude plane for u' at 60S (band-passed filtered to remove inter-annual fluctuations that may be associated with changing boundary conditions, and high-frequency noise) exhibits an annular pattern (not shown).

The Northern Hemisphere (NH) is markedly different. At 60N there is a hint of positive cross-planet covariance, but it is not nearly as pronounced as at 60S. This is indicative of the fact that regions separated by 180 degrees of longitude are not significantly correlated

in the NH (Ambaum et al. 2001). This result is insensitive to choice of latitude. We will argue that the fact that the storm track is relatively continuous in the SH compared to the NH allows the eddy feedback to be communicated continuously around a latitude circle, and induce a hemispherically symmetric mode of variability.

Fig. 1 (b) shows the same analysis for the model control run. Again, there is no hemispherically symmetric pulsing of the jet (which resides at 46S in the time-mean), but there is a hemispherically symmetric meridional vacillation of the jet, as indicated by positive cross-planet covariance on the flank of the jet (at 54S). In this regard the model is qualitatively similar to the SH, as may be expected because both have relatively continuous storm tracks.

b. Baroclinically or Barotropically Driven Variability?

Fig. 1 (c) addresses whether PC1 is a baroclinic mode of variability. The solid line shows the correlation coefficient between F_{tot} and PC1 as a function of lead and lag, and is essentially the same as shown in Lorenz and Hartmann (2001). As expected when F_{tot} forces the time derivative of PC1, the strongest positive correlations occur when F_{tot} leads PC1 by a few days. Given that the auto-correlation of F_{tot} drops to zero after just two or three days, the small but positive correlations between F_{tot} and PC1 at positive lags were identified by Lorenz and Hartmann (2001) as a positive feedback between PC1 and F_{tot} , reddening PC1 and giving rise to the dominance of annular modes.

We also show the correlation between H_{tot} and PC1 (dashed line). When H_{tot} leads PC1 there are positive correlations, implying that preceding a poleward displacement of the jet, there is an anomalously strong meridional eddy heat flux at 60S. The peak correlation

between H_{tot} and PC1 leads that between F_{tot} and PC1, consistent with the idea that an anomalously strong heat flux at 60S, or generation of baroclinic eddy activity, precedes the divergence of eddy activity aloft and associated momentum flux convergence that drives PC1 positive. At zero lag the eddy heat flux is not latitudinally displaced, likely because the meridional temperature gradient in the region of 60S is diminished at zero lag following the increased heat flux a few days previously. However, the correlation does not drop below zero, and at positive lags there is again a positive heat flux anomaly at 60S. This is indicative that a baroclinic feedback may enhance the temperature gradient at the latitude of the anomalous wind-speed maximum (causing the increased heat flux).

Limpasuvan and Hartmann (2000) looked at the regression of the EP flux vector onto PC1 at zero lag. They found no anomalous wave source at 60S associated with a positive PC1, but simply anomalous propagation aloft, thereby suggesting a barotropic mechanism. However, it is clear from Fig. 1 (c) that if the EP flux anomaly were averaged over e.g. lag -7 to lag +7, there would be an anomalous heat flux (and so source of wave activity) at 60S associated with a positive PC1. Subsequent meridional eddy propagation must drive an increase in the barotropic wind-speed that sustains the annular mode. Fig. 1(d) shows the same analysis for the model control run. The correlation coefficients are higher at all lead/lags, but the basic behaviour is the same. The increased correlations in the model may be because the model is dry and the forcings steady in time, so that any underlying eddy-mean flow feedbacks are strong and not diminished by stochastic noise to the same extent as in the real atmosphere. Again, the positive correlations with H_{tot} imply that a positive PC1 is associated with increased heat flux poleward of its climatological position. The reduction in H_{tot} occurs at zero lag, but it remains positive. Thus it appears to be simply

coincidental that in the observations H_{tot} drops to approximately zero (and so there is no anomalous source of eddy activity) at zero lag, rather than due to fundamental dynamics. When the temperature gradient at 60S was regressed onto PC1 (not shown), it increases at small positive lags, implying that the meridional temperature gradient is dynamically enhanced at the anomalous jet core, consistent with $H_{tot} > 0$ at positive lags.

Lorenz and Hartmann (2001) showed that the power spectrum of PC1 is red. They also showed that the power spectrum of F_{tot} is red only due to contributions from F_{hf} . This fact was used to argue that the large scale u anomalies must organise the high-frequency eddies, indicative of a positive feedback between the mean flow and the high-frequency eddies. The power spectrum of F_{hf} is shown in Fig. 1 (e) for the observations, and Fig 1 (f) for the model control run. Also shown is the power spectrum of H_{hf} . Both F_{hf} and H_{hf} exhibit power at the longest time scales. Because the model forcings are steady in time, a strong statement can be made that the high-frequency heat flux must be organised by the mean flow, reddening H_{hf} . $H_{hf} \neq 0$ corresponds to a change in the eddy source latitude, and must cause the barotropic jet to change latitude. In this metric, and in the behaviour of H_{tot} , the annular modes are seen to be a baroclinic mode of variability. Given that the observational data exhibit such similar behaviour, it appears that the same statement can be made about the real atmosphere.

[Figure 1 about here.]

c. Baroclinic Feedbacks in the Simplified GCM

We now turn our attention to the question of whether the model exhibits the hypothesized eddy-driven thermally indirect circulation that encourages the largest meridional temperature gradients to be co-located with the eddy-driven jet. This is easier to evaluate in the model first, because latent heating provides an additional complication in the real atmosphere, and because one can change parameters in the simplified GCM and evaluate the effects on the simulated annular modes. The meridional temperature gradient averaged over the lower half of the model domain is shown in Fig. 2 (a) for the equilibrium temperature (∇T_{eq}) and the output temperature of the run (∇T). ∇T is less than ∇T_{eq} at all latitudes, consistent with the fact that eddies are generated through baroclinic instability and the poleward transport of heat. ∇T_{eq} exhibits a broad maximum in the mid-latitudes. In comparison ∇T has a much more sharply peaked maximum. The eddy heat flux convergence is shown in Fig. 2 (b) and shows that in the lower atmosphere the transport of heat by the eddies acts primarily to cool the region 20-30S and heat the region 50-60S, which would act to reduce the temperature gradient at 40S. The mid-latitude node of the eddy heat flux convergence can be taken as the location of the storm track or eddy driven jet. The temperature gradient is reduced least effectively where the direct transport of heat by the eddies acts to reduce it the most. The same phenomena whereby ∇T is a maximum at the latitude of the storm track was also observed in Panetta (1993) and references therein, and appears to be a fundamental feature of baroclinically unstable planetary atmospheres. When the model was run in a zonally-symmetric configuration, with no eddies, ∇T was a little less than ∇T_{eq} , but qualitatively similar, with a broad maximum in mid-latitudes (not shown). So the net effect

of the eddies is to reduce ∇T everywhere, but they do so least effectively where they are most active. This is consistent with the notion that there exists an eddy-driven thermally indirect meridional overturning that transports enough heat to significantly offset the direct effect of the eddies at the jet core, giving the jet some degree of self-maintenance.

The positive baroclinic feedback can be seen in the climatology of \bar{w}^* . $\bar{w}^* > 0$ on the poleward flank of the eddy-driven jet, with $\bar{w}^* < 0$ on the equatorward flank is indicative of a local Lagrangian thermally indirect circulation. If the thermally indirect circulation flanks the jet core, it may offset the direct effect of the eddy heat flux to the extent that the temperature gradient is reduced least effectively at the jet core, and encourage further baroclinic growth. As described above, Robinson (2006) and Gerber and Vallis (2007) argued that a local maximum in $\nabla \cdot \vec{F}$ in the upper atmosphere at the jet core must lead to such motion. On the other hand, Edmon et al. (1980) proposed that the observed $\bar{w}^* > 0$ in the mid-latitudes may be due to latent heating and the divergence of the vertical transport of heat by baroclinic eddies. \bar{w}^* for the model control run (Fig. 2 (c)) shows rising on the poleward flank of the jet and sinking on the equatorward flank of the jet, and is consistent with the local maximum in $\nabla \cdot \vec{F}$ in the storm track in this model (Gerber and Vallis (2007) their Fig. 12). This rising motion gives the characteristic “U” shape in the T.E.M streamfunction in the mid-latitudes, identified by Robinson (2006) as necessary for a self-maintaining eddy-driven jet. To address the proposal in Edmon et al. (1980) that this “U” may be due to the divergence of the vertical eddy heat flux, $\frac{\partial}{\partial z} \overline{w'T'}$ is shown in Fig. 2 (d). The spatial pattern of the thermally indirect \bar{w}^* does not match that of $\frac{\partial}{\partial z} \overline{w'T'}$, which is a maximum at the jet core, and so we conclude that the rising on the poleward flank of the jet is not due solely to $\frac{\partial}{\partial z} \overline{w'T'}$. Given that there is no latent heating, this is indicative of a

baroclinic feedback in this model.

[Figure 2 about here.]

If the annular mode is due to the meridional wanderings of a self-maintaining jet, it is expected that the characteristic time scale, the e -folding period for the auto-correlation of PC1, would be increased when the self-maintenance mechanism is stronger. To investigate this we present a suite of experiments where ∇T_{eq} is kept the same in the troposphere, but other parameters were varied in the hope of changing the strength of the feedback. The strength of the baroclinic feedback is expected to vary with the magnitude of the local maximum of $\nabla \cdot \vec{F}$ in the upper atmosphere. This depends on the profile of $\frac{\partial}{\partial y} \overline{u'v'}$, which can be altered by changing e.g. the separation between eddy source and sink latitudes (Robinson 2006). Therefore it is expected that the strength of the feedback will vary with changes in mean state that affect the zonal wind-speed climatology, or the eddy length scale (which affects propagation characteristics) and in turn the location of critical latitudes where eddies are dissipated. To this end, experiments were conducted with changes to (i) the tropopause height, (ii) the spatial scale at which energy was removed from the model, (iii) the e -folding time for Newtonian friction, and (iv) the static stability. The caption of Fig. 3 details the specific changes in forcing for each run. Given that ∇T_{eq} is kept the same for each simulation, the maximum value of ∇T for each run is related to the strength of the baroclinic feedback; when there is more self-maintenance, the maximum value of ∇T ($\max(\nabla T)$) should be higher as more heat is transported in a thermally indirect sense. Fig. 3 (a) shows the e -folding time for PC1 for the different experiments as a function of $\max(\nabla T)$. Although it is not expected that the relationship be simple and linear, there is a clear positive correlation between the

e -folding time of PC1 and $\max(\nabla T)$. This is taken as further evidence that the annular mode in this model is a result of a baroclinic feedback, and that the stronger that feedback, the more persistent the annular mode. When the feedback is strong, the self-maintaining jet can wander to latitudes away from where the diabatic forcing acts to generate maximum baroclinic instability, and can remain displaced for long periods of time.

Fig. 3 (b) shows $\max(\nabla T)$ on the ordinate for each model run and $\sum \bar{w}_{eddy} * N^2$ on the poleward flank of the jet on the abscissa. There is a clear negative relationship, indicating that variations in the eddy-driven thermally indirect circulation (and thus the strength of the baroclinic feedback) are likely responsible for the variations in $\max(\nabla T)$. Fig 3 (c) shows the e -folding time as a function of the $\sum \bar{w}_{eddy} * N^2$ on the poleward flank, confirming the deduction that can be made from Figs. 3 (a) and (b) that a stronger eddy-driven thermally indirect overturning is associated with a more persistent PC1. Fig 3 (d) shows $\max(\nabla T)$ on the ordinate and $\sum -\frac{\partial}{\partial y} \overline{v'T'}$ on the abscissa, showing that variations in the direct eddy transport of heat are not responsible for variations in $\max(\nabla T)$. This is expected to be a conservative relationship anyway, because as ∇T increases, the eddy heat flux would be expected to increase to reduce ∇T .

[Figure 3 about here.]

d. Baroclinic Feedbacks in Observations

We now address whether a similar mechanism appears to be important in the real atmosphere. The climatology for \bar{w}^* in the SH is shown in Fig. 4 (a). Consistent with the “U” shaped T.E.M. streamfunction in Edmon et al. (1980), $\bar{w}^* > 0$ in the mid-latitudes.

Also shown in Fig. 4 (a) is $-\frac{1}{f}\nabla \cdot \vec{F}$ averaged from 300 hPa to 20 hPa, which in steady state is equal to the T.E.M. northward meridional velocity (\bar{v}^*). The observed profile of $-\frac{1}{f}\nabla \cdot \vec{F}$ between 55S and 45S is expected to drive rising motion below 300 hPa at those latitudes, as is observed. However, in addressing whether this rising motion constitutes the same positive baroclinic feedback diagnosed in the model, it is also important to consider the latent heating ($\frac{\partial T}{\partial t}|_{latent}$). The climatology of ($\frac{\partial T}{\partial t}|_{latent}$) is shown in Fig. 4 (b), along with the zero contour of \bar{w}^* (from Fig. 4 (a)). There is a maximum in the storm-track, nearly coincident with $\bar{w}^* > 0$, and so we cannot conclude that the region of $\bar{w}^* > 0$ in the observed climatological mean is eddy-driven in the sense discussed above.

[Figure 4 about here.]

An alternative approach is to examine the variability of \bar{w}^* . Fig. 5 (a) shows the regression coefficient for \bar{w}^* and PC1. The tripolar pattern of the \bar{w}^* anomalies is expected for a poleward shift of a single thermally indirect cell. The \bar{w}^* anomalies are nearly, although not quite, in quadrature with the u anomalies, which are maximum (minimum) at 60S (40S). Given that the changes in \bar{w}^* are primarily below 300 hPa, we also show the regression coefficient of $\frac{1}{f}\nabla \cdot \vec{F}$ averaged from 500-300 hPa, with PC1. The regions where the regression coefficient for $\frac{1}{f}\nabla \cdot \vec{F}$ increases towards the equator (and is expected to drive rising motion below) correspond well to the regions of anomalous $\bar{w}^* > 0$.

The regression coefficient for $\frac{\partial T}{\partial t}|_{latent}$ and PC1 is shown in Fig. 5 (b). When the eddy-driven jet is displaced poleward there is increased latent heating at 60S and decreased latent heating at 50-40S. The spatial pattern of the \bar{w}^* anomalies is not consistent with being solely due to the $\frac{\partial T}{\partial t}|_{latent}$ anomalies, and we conclude that the \bar{w}^* anomalies must be

at least partly eddy driven, as suggested by the $\frac{1}{f}\nabla \cdot \vec{F}$ anomalies. The \bar{w}^* anomalies are not quite in quadrature with the u anomalies. This is likely because the $\frac{\partial}{\partial t}T|_{latent}$ anomalies contribute to \bar{w}^* anomalies at the core of the jet. \bar{w}^* anomalies in quadrature with the u anomalies constitute a positive baroclinic feedback, as diagnosed in the model output above. A large portion of the \bar{w}^* anomalies associated with a positive PC1 are in quadrature with the associated u anomalies, and so it appears that there is a baroclinic feedback, which would act to redden the power spectrum of PC1. The diabatic heating processes in the real atmosphere are complicated, and it is perhaps not surprising that the \bar{w}^* associated with a positive baroclinic feedback cannot be definitively ascertained from the climatological picture. However, examining the variability of \bar{w}^* has revealed that such a feedback is manifest in the real atmosphere. Quantifying the importance of this feature is the subject of ongoing work.

[Figure 5 about here.]

4. Discussion and Conclusions

We have examined the characteristics of the leading mode of extra-tropical circulation variability in the context of recent theories that a positive baroclinic feedback results in the self-maintenance of eddy-driven jets (Robinson 2006) and discourages the latitudinal movement of the jet (Gerber and Vallis 2007). Given that the equivalent-barotropic westerlies are a consequence of there being a net eddy source region (Held 1975), it may be expected that their variability be associated with changes in the eddy source region. A time series of

the latitudinal displacement of the high-frequency eddy heat flux was shown to have most power at the longest time-scales, implying that generation of high-frequency eddies must be organised by the mean flow. When the jet is displaced poleward, so is the eddy heat flux, implying that eddies are generated poleward of the climatological position. Meridional propagation of these eddies aloft encourages the jet to remain displaced. This feedback is expected if baroclinic eddies tend to be born at the latitude of the eddy-driven jet stream. This in turn is expected if there exists a thermally indirect circulation that ensures that the largest meridional temperature gradient (and thus baroclinic instability) occurs at the jet core. It was first argued by Robinson (2006) that such a circulation follows from a local maximum in $\frac{1}{f}\nabla \cdot \vec{F}$ at the core of the jet in the upper troposphere. Then, by the conservation of mass and the principle of downward control, in the T.E.M. circulation there must be thermally indirect rising and cooling on the poleward flank of the jet and sinking and warming on the equatorward flank. We have shown that the strength of this circulation is directly related to the time-scale for persistence of the annular mode in a GCM, and appears to be important in the real atmosphere.

In this metric the annular modes are seen to be fundamentally the variability of a baroclinic storm-track, as discussed in e.g. Vallis and Gerber (2008). Because there is a degree of self-maintenance the storm track can wander meridionally for prolonged periods. From this point of view it is not surprising that the Northern Hemisphere does not exhibit genuine zonal symmetry, whereas the Southern Hemisphere does, because the storm-track in the Northern Hemisphere is broken by the existence of continents. It also is expected that down-stream regions of a longitudinally localised storm-track exhibit the maximum variance, as this is where the eddies from upstream can influence where new eddies are most likely to

be generated.

It is worth considering whether this baroclinic feedback is a fundamental feature of atmospheric circulation. From the arguments outlined above, the feedback is a result of the convergence of the meridional flux of momentum (due to meridional wave propagation) being confined to a narrower latitude band than the divergence of the downward flux of momentum (due to the heat flux form drag). Over a hemisphere, the meridionally-propagating eddies must have both source and sink (dissipation) latitudes, whereas the heat flux is generally one sign. So it is expected that the meridional momentum flux term has sharper meridional gradients than the vertical heat flux term. This means that the EP flux divergence will tend to have a local maximum where the meridional momentum flux term is maximum (at the core of the jet in the upper atmosphere) and the self-maintaining flow may be a feature that occurs in baroclinically unstable planetary atmospheres over a wide range of conditions. Indeed, these same dynamics may also be the cause of latitudinally localised storm-tracks in what would be a broad baroclinically unstable zone in the absence of a positive baroclinic feedback.

REFERENCES

- Ambaum, M. H. P., B. J. Hoskins, and D. B. Stephenson, 2001: Arctic oscillation or north atlantic oscillation? *Journal of Climate*, **14 (16)**, 3495–3507.
- Baldwin, M. P., 2001: Annular modes in global daily surface pressure. *Geophysical Research Letters*, **28 (21)**, 4115–4118.
- Bengtsson, L., K. I. Hodges, and E. Roeckner, 2006: Storm tracks and climate change. *Journal of Climate*, **19 (15)**, 3518–3543.
- Cash, B. A., P. J. Kushner, and G. K. Vallis, 2005: Zonal asymmetries, teleconnections, and annular patterns in a gcm. *Journal of the Atmospheric Sciences*, **62 (1)**, 207–219.
- Edmon, H., B. Hoskins, and M. McIntyre, 1980: Eliassen-palm cross sections for the troposphere. *Journal of the Atmospheric Sciences*, **37 (12)**, 2600–2616.
- Gerber, E. P. and G. K. Vallis, 2007: Eddy-zonal flow interactions and the persistence of the zonal index. *Journal of the Atmospheric Sciences*, **64 (9)**, 3296–3311.
- Gillett, N. P., T. D. Kell, and P. D. Jones, 2006: Regional climate impacts of the southern annular mode. *Geophysical Research Letters*, **33 (23)**.
- Gong, D. Y. and S. W. Wang, 1999: Definition of antarctic oscillation index. *Geophysical Research Letters*, **26 (4)**, 459–462.

- Hartmann, D. L., 1995: A pv view of zonal flow vacillation. *Journal of the Atmospheric Sciences*, **52** (14), 2561–2576.
- Hartmann, D. L., 2000: The key role of lower-level meridional shear in baroclinic wave life cycles. *Journal of the Atmospheric Sciences*, **57** (3), 389–401.
- Haynes, P. H., M. E. McIntyre, T. G. Shepherd, C. J. Marks, and K. P. Shine, 1991: On the downward control of extratropical diabatic circulations by eddy-induced mean zonal forces. *Journal of the Atmospheric Sciences*, **48** (4), 651–678.
- Held, I. M., 1975: Momentum transport by quasi-geostrophic eddies. *Journal of the Atmospheric Sciences*, **32**(7), 1494–1497.
- Held, I. M. and M. J. Suarez, 1994: A proposal for the intercomparison of the dynamical cores of atmospheric general circulation models. *Bulletin of the American Meteorological Society*, **75** (10), 1825–1830.
- Holton, J., 1992: *An Introduction to Dynamic Meteorology*. Academic Press.
- Hurrell, J., Y. Kushnir, G. Ottersen, and M. Visbeck, 2003: The north atlantic oscillation: Climate significance and environmental impact. *Geophysical Monograph Series*, **134**, 279.
- Huth, R., 2007: Arctic or north atlantic oscillation? arguments based on the principal component analysis methodology. *Theoretical and Applied Climatology*, **89** (1-2), 1–8.
- Kalnay, E., et al., 1996: The ncep/ncar 40-year reanalysis project. *Bulletin of the American Meteorological Society*, **77** (3), 437–471.

- Kidson, J. W., 1988: Interannual variations in the southern hemisphere circulation. *Journal of Climate*, **1**, 1177–1198.
- Kushner, P. J., I. M. Held, and T. L. Delworth, 2001: Southern hemisphere atmospheric circulation response to global warming. *Journal of Climate*, **14** (10), 2238–2249.
- Limpasuvan, V. and D. L. Hartmann, 1999: Eddies and the annular modes of climate variability. *Geophysical Research Letters*, **26** (20), 3133–3136.
- Limpasuvan, V. and D. L. Hartmann, 2000: Wave-maintained annular modes of climate variability. *Journal of Climate*, **13** (24), 4414–4429.
- Lorenz, D. J. and D. L. Hartmann, 2001: Eddy-zonal flow feedback in the southern hemisphere. *Journal of the Atmospheric Sciences*, **58** (21), 3312–3327.
- Lorenz, D. J. and D. L. Hartmann, 2003: Eddy-zonal flow feedback in the northern hemisphere winter. *Journal of Climate*, **16** (8), 1212–1227.
- Marshall, J., et al., 2001: North atlantic climate variability: Phenomena, impacts and mechanisms. *International Journal of Climatology*, **21** (15), 1863–1898.
- Matsueda, M. and H. L. Tanaka, 2005: Eof and svd analyses of the low-frequency variability of the barotropic component of the atmosphere. *Journal of the Meteorological Society of Japan*, **83** (4), 517–529.
- Meehl, G. T. S., et al., 2007: *Global Climate Projections. In: Climate Change 2007: The Physical Science Basis. Contribution of Working Group I to the Fourth Assessment Report*

of the Intergovernmental Panel on Climate Change. Cambridge University Press, Cambridge, United Kingdom and New York, NY, USA.

Miller, R. L., G. A. Schmidt, and D. T. Shindell, 2006: Forced annular variations in the 20th century intergovernmental panel on climate change fourth assessment report models. *Journal of Geophysical Research-Atmospheres*, **111** (D18).

Mo, K. C. and G. H. White, 1985: Teleconnections in the southern hemisphere. *Monthly Weather Review*, **113** (1), 22–37.

Panetta, R. L., 1993: Zonal jets in wide baroclinically unstable regions: Persistence and scale selection. *Journal of the Atmospheric Sciences*, **50** (14), 2073–2106.

Ring, M. J. and R. A. Plumb, 2007: Forced annular mode patterns in a simple atmospheric general circulation model. *Journal of the Atmospheric Sciences*, **64** (10), 3611–3626.

Robinson, W. A., 1994: Eddy feedbacks on the zonal index and eddy zonal flow interactions induced by zonal flow transience. *Journal of the Atmospheric Sciences*, **51** (17), 2553–2562.

Robinson, W. A., 1996: Does eddy feedback sustain variability in the zonal index? *Journal of the Atmospheric Sciences*, **53** (23), 3556–3569.

Robinson, W. A., 2000: A baroclinic mechanism for the eddy feedback on the zonal index. *Journal of the Atmospheric Sciences*, **57** (3), 415–422.

Robinson, W. A., 2006: On the self-maintenance of midlatitude jets. *Journal of the Atmospheric Sciences*, **63** (8), 2109–2122.

- Seager, R., N. Harnik, Y. Kushnir, W. Robinson, and J. Miller, 2003: Mechanisms of hemispherically symmetric climate variability. *Journal of Climate*, **16** (18), 2960–2978.
- Simmons, A. J. and B. J. Hoskins, 1978: The life cycles of some nonlinear baroclinic waves. *Journal of the Atmospheric Sciences*, **35** (3), 414–432.
- Thompson, D., S. Lee, and M. P. Baldwin, 2003: Atmospheric processes governing the northern hemisphere annular mode/ north atlantic oscillation. *Geophysical monograph*, **x**, x.
- Thompson, D. W. J. and J. M. Wallace, 1998: The arctic oscillation signature in the wintertime geopotential height and temperature fields. *Geophysical Research Letters*, **25** (9), 1297–1300.
- Thompson, D. W. J. and J. M. Wallace, 2000: Annular modes in the extratropical circulation. part i: Month-to-month variability. *Journal of Climate*, **13** (5), 1000–1016.
- Thompson, D. W. J. and J. M. Wallace, 2001: Regional climate impacts of the northern hemisphere annular mode. *Science*, **293** (5527), 85–89.
- Thorncroft, C. D., B. J. Hoskins, and M. E. McIntyre, 1993: Two paradigms of baroclinic-wave life-cycle behaviour. *Quarterly Journal of the Royal Meteorological Society*, **119** (509), 17–55.
- Vallis, G. K., 2006: *Atmospheric and Oceanic Fluid Dynamics: Fundamentals and Large-Scale Circulation*. Cambridge University Press.
- Vallis, G. K. and E. P. Gerber, 2008: Local and hemispheric dynamics of the north atlantic

- oscillation, annular patterns and the zonal index. *Dynamics of Atmospheres and Oceans*, **44**, 184–212.
- Visbeck, M. H., J. W. Hurrell, L. Polvani, and H. M. Cullen, 2001: The north atlantic oscillation: Past, present, and future. *Proceedings of the National Academy of Sciences of the United States of America*, **98 (23)**, 12 876–12 877.
- Wallace, J. M., 2000: North atlantic oscillation/annular mode: Two paradigms - one phenomenon. *Quarterly Journal of the Royal Meteorological Society*, **126 (564)**, 791–805, part A.
- Wallace, J. M. and D. W. J. Thompson, 2002: The pacific center of action of the northern hemisphere annular mode: Real or artifact? *Journal of Climate*, **15 (14)**, 1987–1991.
- Yin, J. H., 2005: A consistent poleward shift of the storm tracks in simulations of 21st century climate. *Geophysical Research Letters*, **32**, 1–4.

List of Figures

1	The left column shows data from the NCEP reanalysis and the right column shows output from the model control run. The top panels show the ‘cross-planet cospectrum’ (see text) for zonal wind-speed anomalies at 300 hPa. The central panels show the lead/lag correlation coefficient (R) between PC1 (see text), the momentum flux forcing F_{tot} (see text) and the poleward displacement of the eddy heat flux H_{tot} (see text). The bottom panels show the power spectrum for F_{hf} and H_{hf} (see text), normalised so that the maximum spectral density is unity.	31
2	Model control run diagnostics. (a) The meridional gradient of the equilibrium temperature (∇T_{eq}) and the output temperature (∇T) averaged over the lower half of the model domain. (b) The climatological transformed Eulerian mean (T.E.M.) vertical velocity (\bar{w}^* , see text). (c) The convergence of the meridional eddy heat flux ($-\frac{\partial}{\partial y}\overline{v'T'}$). (d) The climatological divergence of the vertical eddy heat flux ($\frac{\partial}{\partial z}\overline{w'T'}$)	32

- 3 Comparison of a suite of model runs. Relative to the control run, in the H-S experiments, the subscripted value in the legend was added to T_{eq} at the tropopause and stratosphere, and decreased to zero at the surface. In the Del experiments, the power of the hyperdiffusivity operator was changed to the superscripted value. In the Tstrat experiments T_{eq} in the stratosphere was changed to the succeeding value. In the TFRC experiments the e -folding time of the linear drag operator was changed to the succeeding value. (a) The e -folding period of PC1 on the ordinate and the maximum value of ∇T ($\max(\nabla T)$) on the abscissa. (b) ($\max(\nabla T)$) on the ordinate and the sum of the eddy-driven thermally indirect cooling ($\sum \bar{w}^* N^2$, see text) on the abscissa. (c) e -folding period of PC1 on the ordinate and $\sum \bar{w}^* N^2$ on the abscissa. (d) ($\max(\nabla T)$) on the ordinate and $\sum -\frac{\partial \overline{v'T'}}{\partial y}$ on the poleward flank of the jet (see text) on the abscissa. 33
- 4 (a) The climatological mean \bar{w}^* for the NCEP reanalysis data is shaded with the zero contour bolded. The dashed line shows the T.E.M. meridional velocity required to balance the Eliassen-Palm flux divergence ($\frac{1}{f}\nabla \cdot \vec{F}$), see text). (b) the climatological mean temperature tendency due to latent heating ($\frac{\partial T}{\partial t}|_{latent}$). Also shown is the zero contour from panel (a). 34
- 5 (a) The regression coefficient for \bar{w}^* for the NCEP reanalysis data and PC1 is shaded. The dashed line shows the regression coefficient for $\frac{1}{f}\nabla \cdot \vec{F}$ averaged between 500-300 hPa and PC1. The solid horizontal line is the zero line for $\frac{1}{f}\nabla \cdot \vec{F}$. (b) The regression coefficient for $\frac{\partial T}{\partial t}|_{latent}$ and PC1. 35

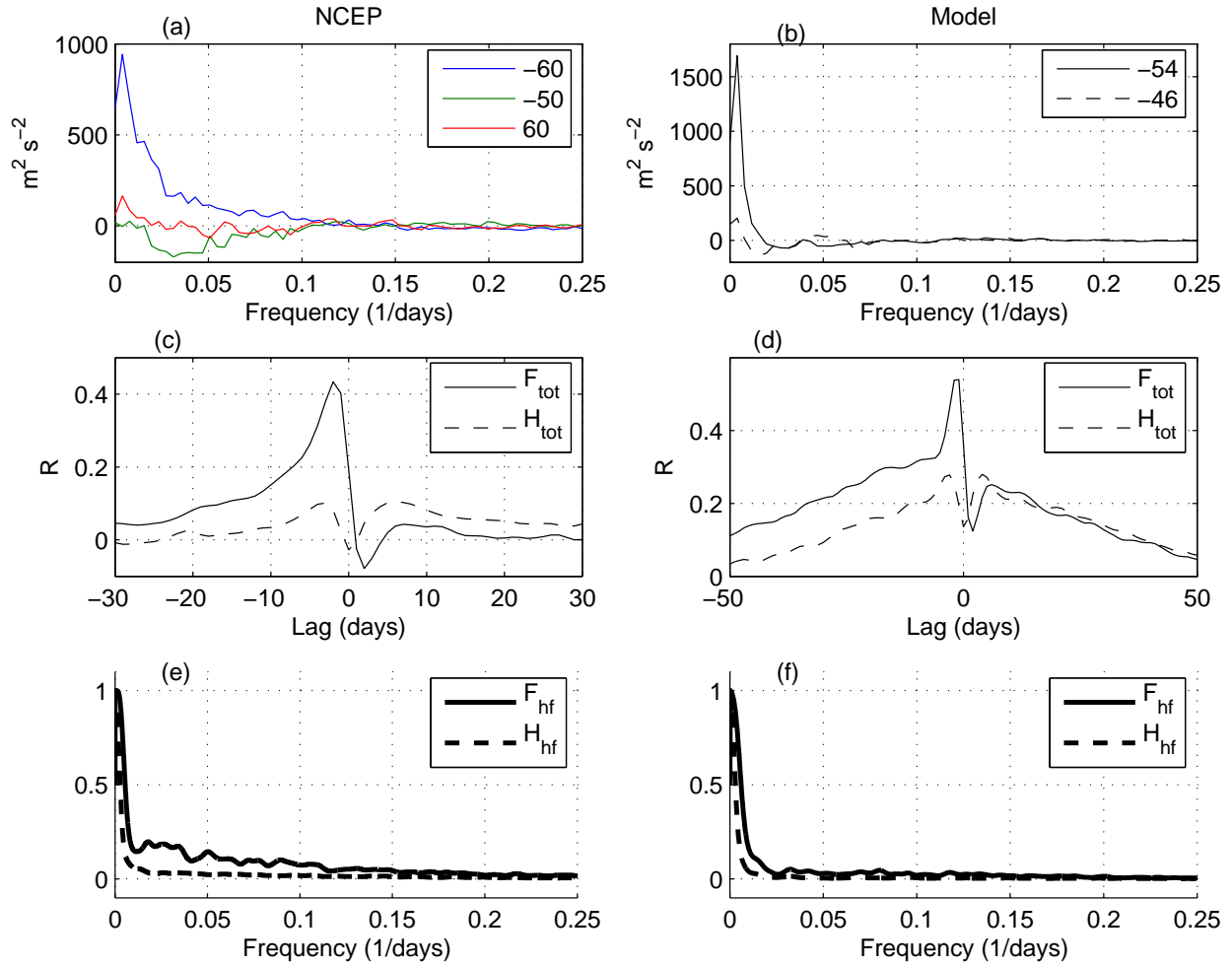


FIG. 1. The left column shows data from the NCEP reanalysis and the right column shows output from the model control run. The top panels show the ‘cross-planet cospectrum’ (see text) for zonal wind-speed anomalies at 300 hPa. The central panels show the lead/lag correlation coefficient (R) between PC1 (see text), the momentum flux forcing F_{tot} (see text) and the poleward displacement of the eddy heat flux H_{tot} (see text). The bottom panels show the power spectrum for F_{hf} and H_{hf} (see text), normalised so that the maximum spectral density is unity.

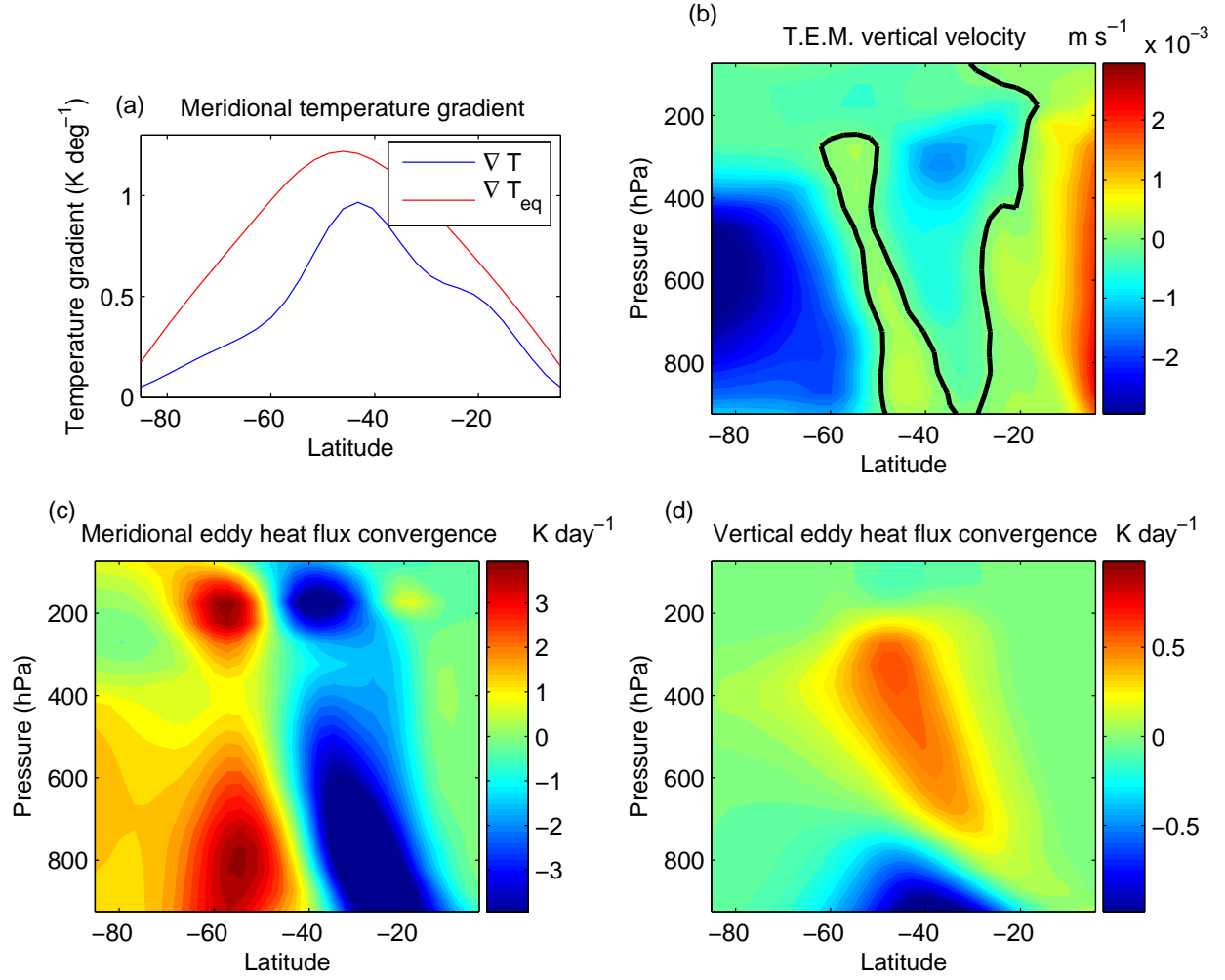


FIG. 2. Model control run diagnostics. (a) The meridional gradient of the equilibrium temperature (∇T_{eq}) and the output temperature (∇T) averaged over the lower half of the model domain. (b) The climatological transformed Eulerian mean (T.E.M.) vertical velocity (\bar{w}^* , see text). (c) The convergence of the meridional eddy heat flux ($-\frac{\partial}{\partial y} \overline{v'T'}$). (d) The climatological divergence of the vertical eddy heat flux ($\frac{\partial}{\partial z} \overline{w'T'}$)

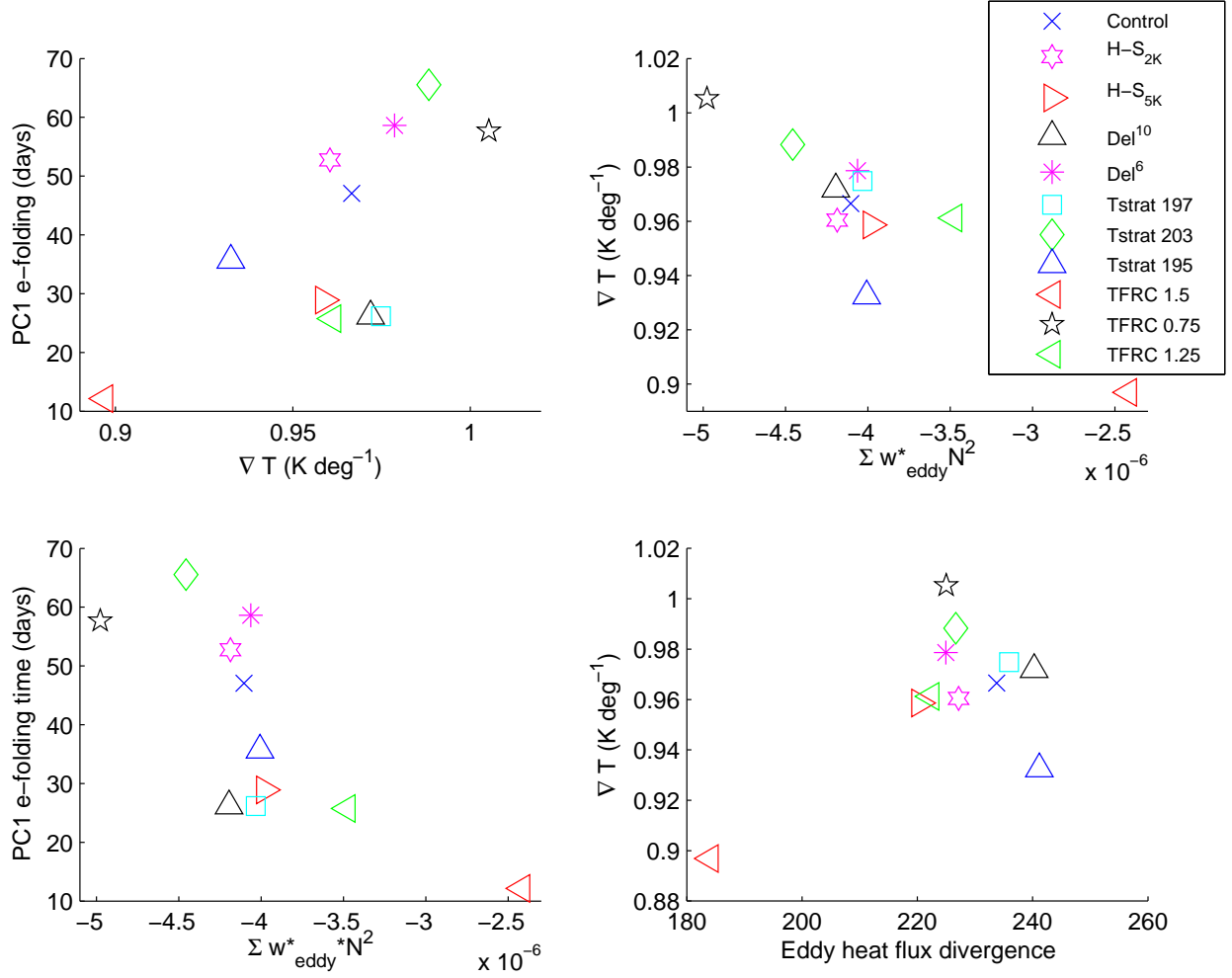


FIG. 3. Comparison of a suite of model runs. Relative to the control run, in the H-S experiments, the subscripted value in the legend was added to T_{eq} at the tropopause and stratosphere, and decreased to zero at the surface. In the Del experiments, the power of the hyperdiffusivity operator was changed to the superscripted value. In the Tstrat experiments T_{eq} in the stratosphere was changed to the succeeding value. In the TFRC experiments the e -folding time of the linear drag operator was changed to the succeeding value. (a) The e -folding period of PC1 on the ordinate and the maximum value of ∇T ($\max(\nabla T)$) on the abscissa. (b) ($\max(\nabla T)$) on the ordinate and the sum of the eddy-driven thermally indirect cooling ($\Sigma \bar{w}^* N^2$, see text) on the abscissa. (c) e -folding period of PC1 on the ordinate and $\Sigma \bar{w}^* N^2$ on the abscissa. (d) ($\max(\nabla T)$) on the ordinate and $\Sigma -\frac{\partial}{\partial y} \bar{v}' T'$ on the poleward flank of the jet (see text) on the abscissa.

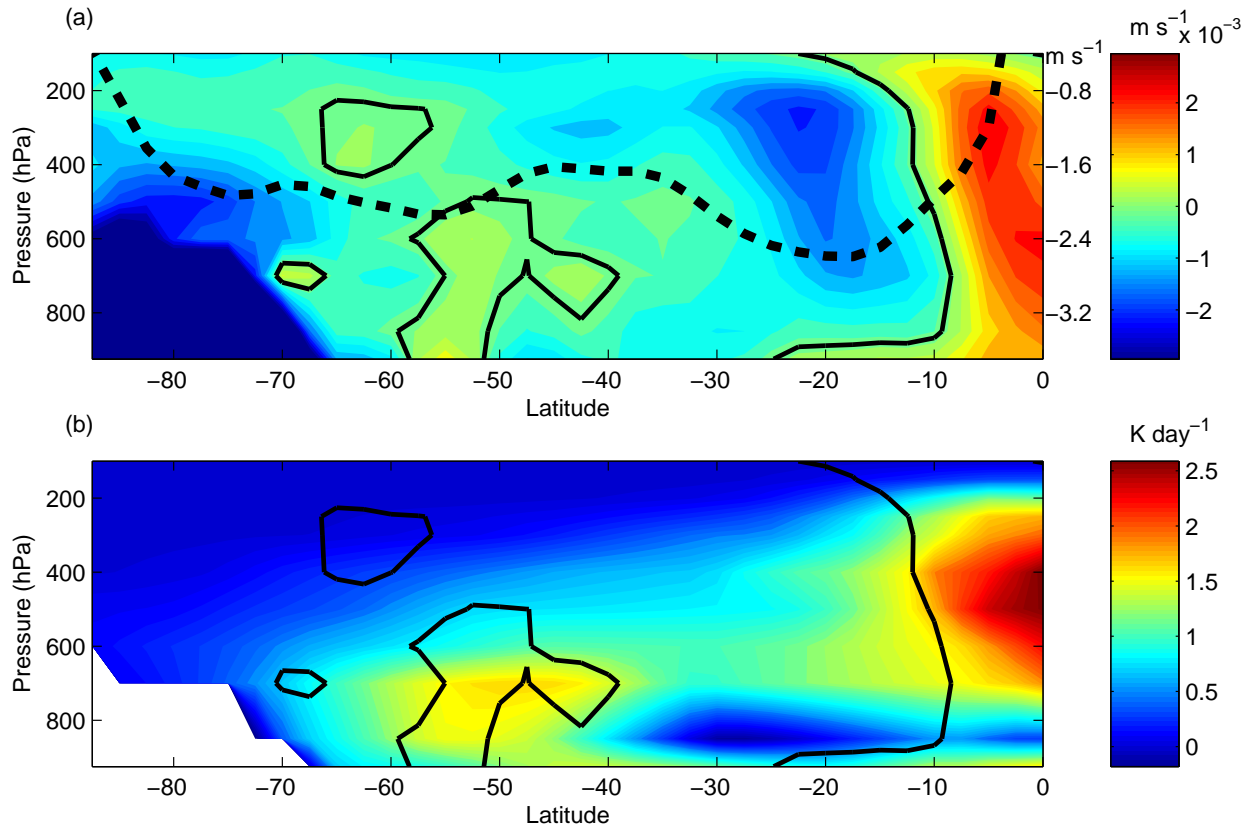


FIG. 4. (a) The climatological mean \bar{w}^* for the NCEP reanalysis data is shaded with the zero contour bolded. The dashed line shows the T.E.M. meridional velocity required to balance the Eliassen-Palm flux divergence ($\frac{1}{f}\nabla \cdot \vec{F}$), see text). (b) the climatological mean temperature tendency due to latent heating ($\frac{\partial}{\partial t}T|_{latent}$). Also shown is the zero contour from panel (a).

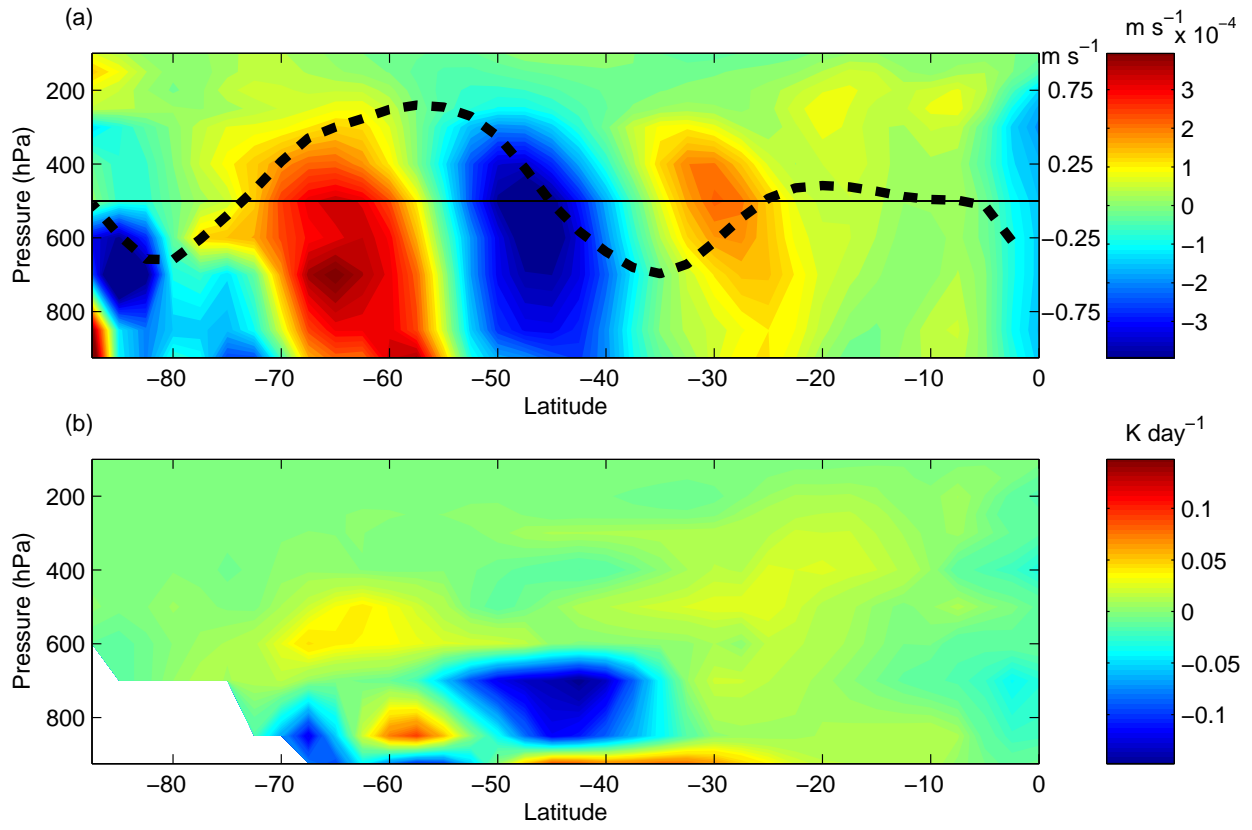


FIG. 5. (a) The regression coefficient for \bar{w}^* for the NCEP reanalysis data and PC1 is shaded. The dashed line shows the regression coefficient for $\frac{1}{f}\nabla \cdot \vec{F}$ averaged between 500-300 hPa and PC1. The solid horizontal line is the zero line for $\frac{1}{f}\nabla \cdot \vec{F}$. (b) The regression coefficient for $\frac{\partial T}{\partial t}|_{latent}$ and PC1.